Comparison of chromium coatings and electrochemical behaviour with direct current and pulse current deposition in trivalent chromium formate urea bath as alternative to conventional Cr coatings

S. Mohan*, G. Saravanan and N. G. Renganathan

Alternative process to hexavalent chromium (Cr) plating, substitute materials and new designs are urgently needed owing to the requirement of 'clean' manufacture. Trivalent Cr coatings with thickness of 29·7 μm, Hardness (HV 1131) and acceptable quality that can be used for wear resistance as well as corrosion resistance purposes were produced successfully in the present work. The results show that the coatings exhibited crack free surface and amorphous/microcrystalline structure. The effect of direct current (DC) and pulse current (PC) on the thickness, hardness and current efficiencies were compared with DC and PC deposition. The Cr coatings were characterised by scanning electron microscope, atomic force microscopy and X-ray diffraction. The morphology of Cr deposits obtained in the formate urea electrolyte is a typical nodular and fine grained structure. As regards to the electrochemical behaviour, the deposited Cr by PC and DC coatings exhibited better corrosion resistance than the mild steel. Therefore, the electroplated Cr coatings are environmentally acceptable to replace the conventional Cr coatings.

Keywords: Trivalent Cr bath, Direct current, Pulse current, Average current, On-time, Off-time, Duty cycle, Urea, Amorphous/microcrystalline, Formate

Introduction

Chromium coatings have been widely used for the decorative and engineering purposes in aerospace, automotive, manufacture industries. Cr coatings provide high hardness, excellent wear, corrosion resistances and strong adhesive ability with substrate.[1,2] Conventional Cr electrodeposited from the hexavalent Cr have been applied for more than 120 years. But nowadays, huge environmental pressures increasingly require that the conventional hexavalent Cr plating process need to be substituted by more environmental friendly technologies for its intense toxicity and carcinogenicity.

Chromium plating from trivalent baths has received renewed interest because of the toxicity of hexavalent Cr ions and the federal regulations on the discharge of hexavalent Cr into waste streams.[3] In the US, commercial decorative trivalent Cr plating processes have been in use since mid-1970. Thick and hard Cr coating with acceptable quality can be electrodeposited successfully from Cr^{3+} bath[4] and few functional researches have been conducted. However, it is almost impossible to deposit the Cr coating from a simple aqueous Cr(III) solution due to a very stable $[Cr(H_2O)_6]^{3+}$ complex. According to the published data[5] the slow deposition rate in Cr(III) sulphate electrolyte is related to the appearance of very stable μ sulphato bridged oligomeric species of Cr(III). To destabilise the strong hexa-aqua Cr (III) complex some of the complexing agents (glycine, urea, acetate, formate, DL Aspartic acid and hypophosphite etc.) may be used.[6–10] The most important fact is that Cr(III) does not oxidise organic compounds. Although the pH in the bulk of the electrolyte may be about 1–2, the diffusion layer pH can reach four. At this pH coordinated water molecules may be converted to OH^- groups, which lead to the formation of μ hydroxo bridged species. This reaction may continue with the formation of large molecules where the Cr atoms are linked with OH^- groups (olated compounds). This is the cause of losses in both the deposition rate and the quality of Cr deposit.[11] The coordinated water molecules, OH^- groups, or other ligands may be replaced by anions in the solution. Anions that easily enter in to the coordinated sphere and displace OH^- groups can effectively prevent olation.[12] Some of organic ligands

Central electrochemical research institute, Karaikudi, Tamilnadu, 630006, India

*Corresponding author, email sanjnamohan@yahoo.com

Published by Maney on behalf of the Institute
Received 12 May 2008; accepted 17 May 2008
DOI 10.1179/174329408X326335

influence the plating rate and the quality of the coatings due to the formation of Cr(III) active complexes. However, the reasons why thick Cr coatings are difficult to obtain from Cr(III) baths have not been fully clarified.

In the present work, comparison of the environmentally acceptable Cr coatings by direct current (DC) and pulse current (PC) with thickness of 39·6 μm, Current efficiency 39·6 Hardness (HV 1131) and acceptable quality were electrodeposited from Cr^{3+} successfully. The microstructure, microhardness and electrochemical behaviour of the electroplated Cr were investigated. Results show that PC Cr deposition has better current efficiency, fine grained, nodular and more microhardness than the DC deposition. It has better corrosion resistance than that of the DC Cr deposit. Therefore, it can be anticipated that the conventional Cr coating will be replaced by the environmentally acceptable Cr coating from trivalent Cr formate urea bath for engineering and decorative purposes.

Experimental

Electrolyte

The bath composition, concentrations and operating conditions for Cr deposition are listed in Table 1. The plating bath uses $Cr_2(SO_4)$ $6H_2O$ as a source of Cr(III) ions, Ammonium formate and urea as complexing agent, $B(OH)_3$ as buffering agent Na_2SO_4, $Al_2(SO_4)_3$ are conducting salts and NaF was used as a wetting agent. Every bath constituent has key role during plating process. All solutions were prepared using double distilled water and AnalaR grade chemicals. The pH was adjusted to 0·6–2·5 with sulphuric acid or potassium hydroxide. After all components were mixed, the solution were heated at 60°C for 20 min, then cooled and aged for 24 h so that the Cr(III) complex formation is completed before deposition. The brass plate was used as substrate and insoluble graphite electrode as anode. The deposition was carried out at 15–30 A dm^{-2}. Current density and the time of deposit is from 15 to 45 min at room temperature. The plates were electrodeposited from trivalent Cr bath by using DC and PC deposition. Pulse plating was conducted using Dynatronix (USA) DPR20-10-5 model. The pulse parameters used are given in Table 2.[13] The Formula used in pulse plating is given below

$$\%\text{duty cycle} = \frac{\text{on time}}{\text{on time} + \text{off time}} \times 100$$

$$\text{Average curren} = \frac{\text{on time}}{\text{total time}} \times \text{peak pulse current}$$

$$\text{Peak current} = \frac{\text{average current}}{\text{duty cycle}} \times 100$$

Electrochemical measurements

Electrochemical experiments were performed using an advanced electrochemical system (Princeton Applied Research, USA) model PARSTAT 2273 at room temperature. The polarisation curves and impedance spectra were obtained in 3·5% NaCl aqueous solution. A three electrode cell was used for electrochemical measurements. The working electrode is the Cr coated by DC and PC on mild steel (Fe–0·07C–0·71Mn–0·11Si–0·013P–0·03Ni–0·01Cr). The counter and reference electrode are a large platinum foil and a saturated calomel electrode (SCE) respectively. Measurement of polarisation curves were carried out at scan rate of 5 mV ms^{-1}, from −0·25 to 0·25 V with respect to open circuit potential. Impedance spectra were recorded for the frequency range from 100 to 10 mHz with the AC amplitude equal to 5 mV ms^{-1}.

Characterisation

Thickness μm of the coatings was measured by using PosiTector 6000 thickness metre. The microstructure, porosity and surface morphology were carried out by scanning electron microscope (SEM) employing a Hitachi 3000H. Structure characterisation of the deposit was carried out by X-ray diffraction (XRD) using a Phillips diffractometer with Cu K (2·2 kW max.) as source. The surface topography of Cr coating was studied using atomic force microscopy (AFM). The basic study comprised a 3D representation for scanned area of 5 × 5 μm. Microhardness of the Cr deposited on brass substrate was evaluated by using a MH6 Everyone hardness tester with Vickers intenders. A dwelling time of 5 s and a load of 50 g were used for the measurement.

Table 1 Composition of trivalent Cr plating bath

Bath composition	Function	Concentration, mol L^{-1}	Operating conditions
$Cr_2(SO_4)$ $6H_2O$	Source of Cr	0·4	Anode: graphite
Na_2SO_4	Conduction salt	0·3	Cathode: brass plate
$Al_2(SO_4)_3$	Conduction salt	0·12	Temperature: 30 ± 2°C
$B(OH)_3$	Buffer agent	0·64	Current density: 15–25 A dm^{-2}
NaF	Wetting agent	0·5	pH: 0·6–2·5
$HCOONH_4$	Complexing agent	0·39	Deposition time: 1–45 min
$(NH_2)_2CO$	Complexing agent	0·74	

Table 2 Pulse parameter used for pulse plating of Cr

	Pulse frequency and pulse on–off times, ms				Current density, A dm^{-2}	
Duty cycle, %	10 Hz	25 Hz	50 Hz	100 Hz	peak	Average
10	10–90	4–36	2–18	1–9	140	14
20	20–80	8–32	4–16	2–8	70	14
40	40–60	16–24	8–12	4–6	35	14
80	80–20	32–8	16–4	8–2	17·5	14

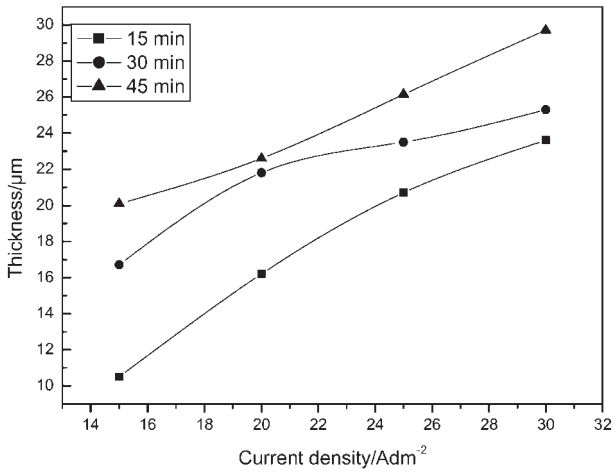

1 Effect of current density on thickness of deposit

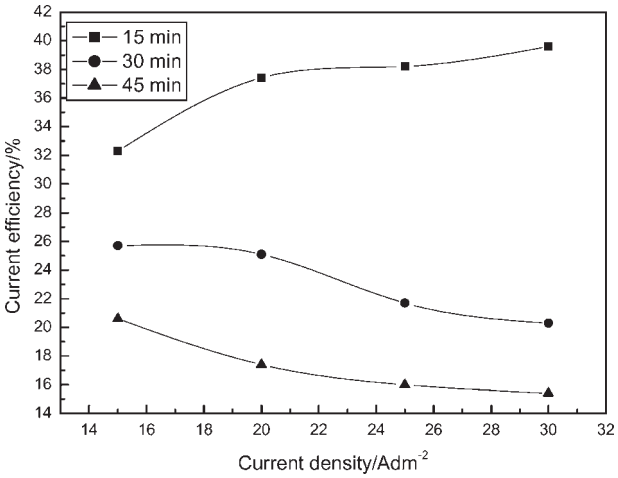

2 Effect of current density on current efficiency of deposit

Results

Comparison of thickness, hardness and current efficiency with direct current electrodeposition

Figure 1 shows the effect of current density and time on thickness of Cr deposit at room temperature. Thickness of the deposit increases with increase in current density from 15 to 30 A dm^{-2} for different time of deposits. Maximum thickness of 29·7 μm is attained for 45 min at 30 A dm^{-2}. From these results the rate of deposition increases with increasing time and current density. It seems clear from the above results that the Cr content in deposits increases gradually with increasing the cathodic current density. The trend with respect to current density suggests that Cr(III) can be electrodeposited better at higher current density but the deposits surface is not smooth with large amounts of cracks. Appearance of glossy nature is lost at higher current densities. In the present case maximum thickness of 29·7 μm has been obtained from this bath and this is more compared to reported value of 12–15 μm at a current density of 7 A dm^{-2}.[14] Here pH limitations are not observed as in the case of above reference where polymerisation and oxidation reactions of Cr(III) complex ion are absent up to higher current density and more thickness could be built up and this is the advantage that can be claimed from the corrosion point of view.

The influence of current density on current efficiency of Cr deposits is shown in Fig. 2. Current efficiency increases with increasing current density and it reaches maximum value of 39·6 for 15 min at 30 A dm^{-2} thereafter current efficiency decreases when increasing time. The current efficiency is maximum of 39·6% as indicated above at the Cr content of 12·1 g L^{-1} and this is little lower compared to 49% at 14·6 g L^{-1}.[15] It is also reported that current efficiency increases with decreasing cathodic pulse time and increasing current time.[16] Increase of current density only to a certain extent will yield good current efficiency which is well brought out from the figure and this is obeyed in a narrow range. This happens for a continued reduction in the cathodic pulse time or an increase of the anodic current density because of the redissolution of Cr. In the absence of complexing agents, the current efficiency is expected to increase with increasing current density. Whereas in presence of complexing agents like formate the current efficiency for hydrogen evolution is expected to be high even at low current density but it goes to lesser extent when the current density is more. Moreover, in the absence of complexing agents Cr deposition does not take place as desired but Cr oxide deposits take place. This suggests that in the presence of suitable complexing agents the Cr reduction must be via the consecutive reactions from a complex Cr^{3+} to Cr(s).

Figure 3 shows the effect of current density and time for hardness of Cr deposition. Hardness increases with increasing current density and time. The maximum hardness of 1131 HV is obtained at 25 A dm^{-2}. The increasing hardness is due to the coating of Cr–C,[17] along with Cr deposition on the substrate. According to the literature report C comes from organic compounds which are used as complexing agents (e.g. ammonium formate and urea). The increasing hardness may also be due to the formation of finer grains at higher current densities which is the case in pulse plating.

Effect of duty cycle on thickness of Cr deposits

Figure 4 shows the effect of pulse duty cycle on the thickness of Cr deposits obtained for various frequencies at 20 A dm^{-2}. From this figure, it is observed that the thickness of the Cr deposit increases with increasing in pulse duty cycle. As the duty cycle increases, current on-time increases and off-time decreases. At a lower duty cycle, the peak current is flowing for less time and so the

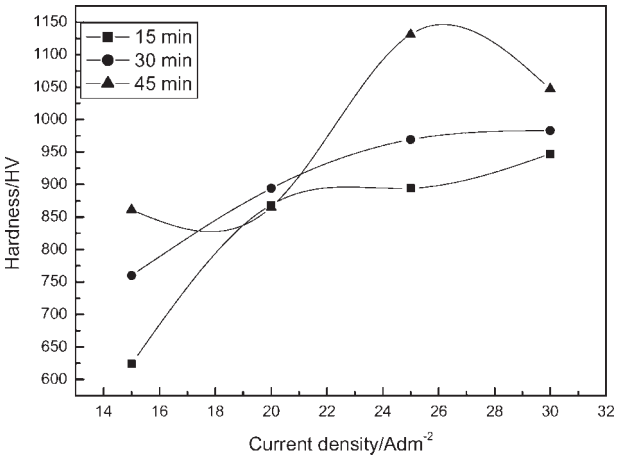

3 Effect of current density on hardness of deposit

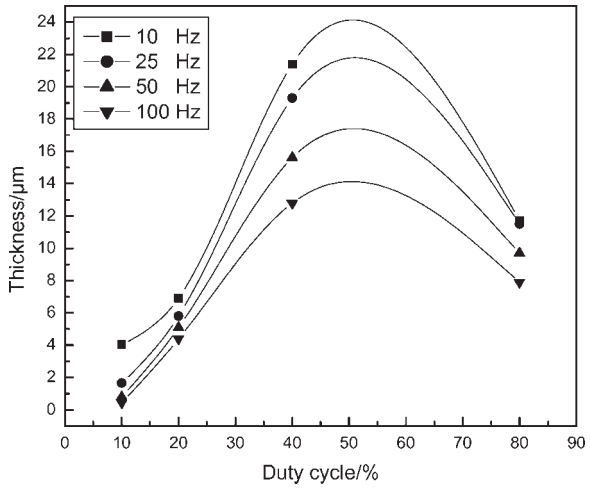

4 Effect of pulse duty cycle on thickness of Cr deposit at 14 A dm^{-2} (AC) at various frequencies

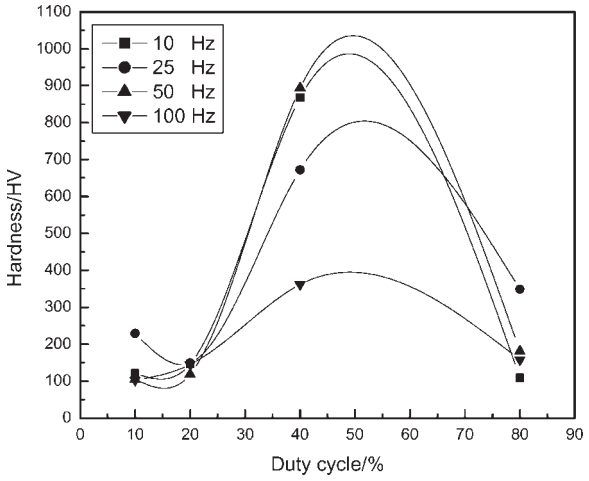

6 Effect of pulse duty cycle on hardness of Cr deposits at 14 A dm^{-2} (AC) at various frequencies

overall amount of deposition is less than for a higher duty cycle. Also at very high duty cycle and high frequencies the pulse current is very low, and so a correspondingly reduced thickness is obtained. The maximum thickness (21·4 μm) was obtained at 40% duty cycle for lower pulse frequencies (10 and 25 Hz) at current density of 20 A dm^{-2}. In pulse current deposition the authors obtained more or less equal thickness as observed in DC deposition even if we use 50% of DC current density.

Effect of pulse duty cycle on current efficiency of Cr deposits

Figure 5 shows the effect of pulse duty cycle on current efficiency of Cr deposits obtained for various frequencies at 20 A dm^{-2}. The maximum current efficiency is obtained at 40% duty cycle at lower pulse frequencies (10 and 25 Hz). As pulse frequency increases, the pulses are very short and they produce very thin pulse diffusion layers. Thus transport and diffusion of metal ions from bulk electrolyte to the cathode surface through these layers is possible and much easier than through the thick diffusion layers, which are obtained at larger pulses. At higher frequencies (100 Hz) favour hydrogen evolution leading to a reduction in current efficiency. Therefore, at

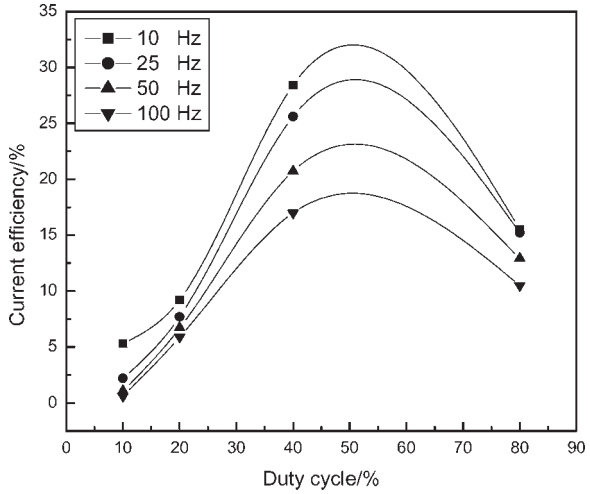

5 Effect of pulse duty cycle on current efficiencies of Cr deposits at 14 A dm^{-2} (AC) at various frequencies

40% duty cycle at lower pulse frequencies enhancement of migration of ions increases the nucleation rate, uniformity of deposit,[18] deposition rate and hence current efficiency is increased.

Effect of pulse duty cycle on hardness of Cr deposits

Figure 6 shows the effect of pulse duty cycle on the hardness of the Cr deposits obtained for various frequencies at 20 A dm^{-2} current density. The hardness of the Cr deposit is found to increase with increase in duty cycle.[19] A maximum hardness value is obtained at 40% duty cycle at low frequencies (10 and 50 Hz) when the current density was 20 A dm^{-2}. Because in a low pulse duty cycle a high peak current is passed, this produces powdery or burnt deposits with poor adhesion and considerable porosity. This porosity leads to a decrease in hardness of the deposit. However, at 40% duty cycle, the peak current is lower to the formation of a smooth fine grained deposit. Improved surface coverage with denser built-up grains is to be expected.[20] At higher frequencies (100 Hz) the pulse current appears to be almost equal to that of DC deposition because there is no sufficient relaxation time for the re-establishment of equilibrium between the ions in the bulk solution and the electrode surface, which leads to the formation of porous deposit. So hardness of the deposit decreases beyond 40% duty cycle.

Potentiodynamic polarisation studies

The principal aim of the present investigation was to study surface degradation resulting from electrochemical processes, and this necessitated in analysis of the surface deposit left after electrochemical reactions. The potentiostatic polarisation experiments provided some idea of the electrochemical activity of the material. However, this necessitated scanning across a wide range of electrode potentials so that the surface of the material at the end of such polarisation was the result of cumulative effects at different potentials. To analyse the surface, the material was subjected to potentiostatic polarisations, one specified potential being impressed on the material at a time.

The potentials were either anodic or cathodic with respect to the primary electrochemical process occurring on the surfaces as indicted by the potentiostatic

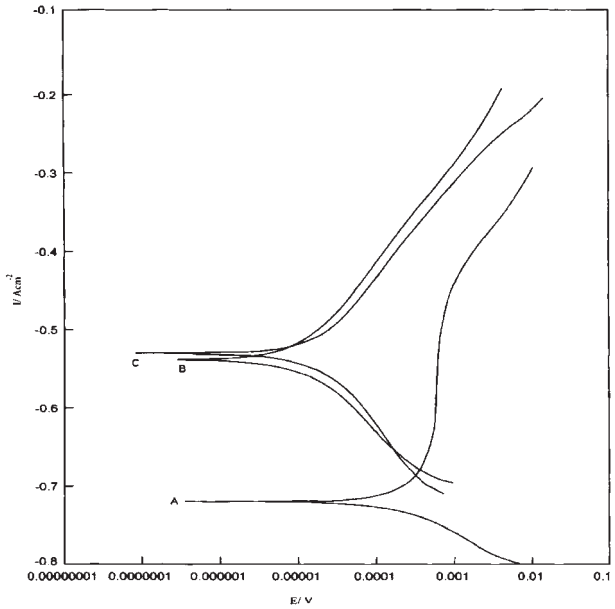

7 Polarisation studies of (A) MS panel, (B) Cr on MS (DC) and (C) Cr on MS (PC) in 3·5% w/v NaCl electrolyte

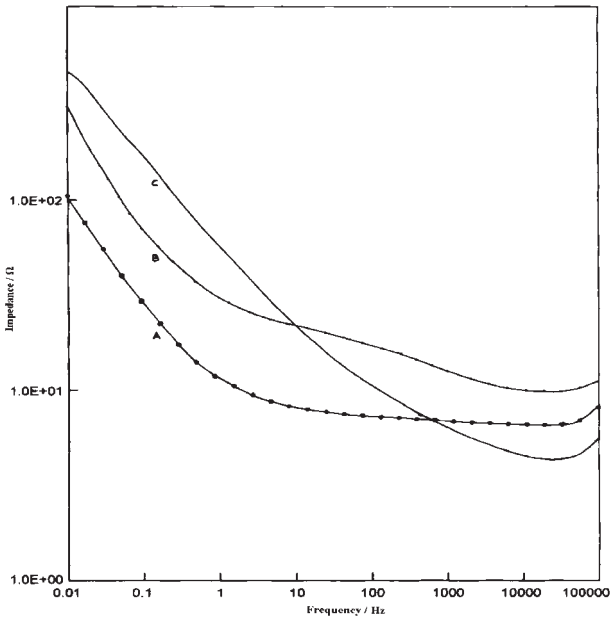

8 Bode plots for corrosion measurement of (A) MS panel, (B) Cr on MS (DC) and (C) Cr on MS (PC) in 3·5%w/v NaCl electrolyte

polarisation curves. The potentiodynamic polarisation curves obtained for the mild steel (substrate), DC deposited, PC plating of Cr (16 μm each) on mild steel in 3·5% w/v NaCl electrolyte are presented in Fig. 7. The current and potential of the corroding electrode is related by

$$i = i_{\text{corr}}(e^{2\cdot3\,\eta/\text{ba}} - e^{2\cdot3\,\eta/\text{bc}})$$

where i_{corr} is corrosion current; η is over potential (E–E_{corr}), b_{a} and b_{c} are anodic and cathodic Tafel slopes.

At high over potentials, i.e.

$$\eta \geqslant RT/F$$

$$i = i_{\text{corr}}\, e^{2\cdot3\,\eta/\text{ba}}$$

$$\log i = \log i_{\text{corr}} + \eta/b_{\text{a}}$$

In the plot of η verses log$i$, extrapolation of linear line to corrosion potential gives a straight line and the slope gives both b_{a} and b_{c} and the intercept gives the corrosion current. The E_{corr} and I_{corr} values have been calculated using the Tafel extrapolation method and they are given in Table 3 and Fig. 7. There is an appreciable increase in corrosion resistance is more for the PC plated and DC deposited Cr than that of bare mild steel substrate. E_{corr} and I_{corr} values improve (a less negative of E_{corr} and lower value of I_{corr} signifies an improvement in corrosion resistance) for both PC plating and DC deposition on mild steel substrate. The E_{corr} values are shifted to near equilibrium/positive value of Cr plating system, which show the reduction of corrosion behaviour of the system.

Electrochemical impedance

The comparative study of electrochemical impedance spectra of DC deposition, PC plating of Cr on mild steel were measured in the same three electrode assembly, as used for the Potentiodynamic polarisation experiments. Impedance measurements were made at open circuit potential (OCP) applying an AC signal of 5 mV ms^{-1} in the frequency range from 100 to 10 mHz. The impedance results obtained from bode plots for the samples used for corrosion tests in 3·5%NaCl solution are shown in Table 4 and Fig. 8.

The R_{ct} can be related to I_{corr}

$$R_{\text{ct}} = b_{\text{a}} \times b_{\text{c}}/2\cdot3(b_{\text{a}} + b_{\text{c}})I_{\text{corr}}$$

R_{sol} solution resistance

R_{ct} charge transfer resistance

b_{a} and $b_{\text{c a}}$ nodic and cathodic Tafel slopes

The double layer capacitance C_{dl} value is obtained from the frequency at which Z imaginary is maximum.

Table 4 Corrosion parameters obtained from impedance measurements by bode plots

sample	OCP, V	R_{ct}, Ω cm^{-2}	C_{dl}, mF cm^{-2}
MS panel	−0·547	102·5	163·4
Cr on MS (DC)	−0·456	233·6	83·02
Cr on MS (PC)	−0·460	812	46·18

Table 3 Corrosion parameters obtained from polarisation studies in 3·5% w/v NaCl electrolyte

Sample	E_{corr} versus SCE, mV	b_{a}, V/decade	b_{c}, V/decade	I_{corr}, A dm^{-2}	Corrosion rate, mils/year
MS panel	−0·720	0·388	−0·056	250	75·9
Cr on MS (DC)	−0·624	0·207	−0·046	14	46
Cr on MS (PC)	−0·532	0·114	−0·113	4·6	15

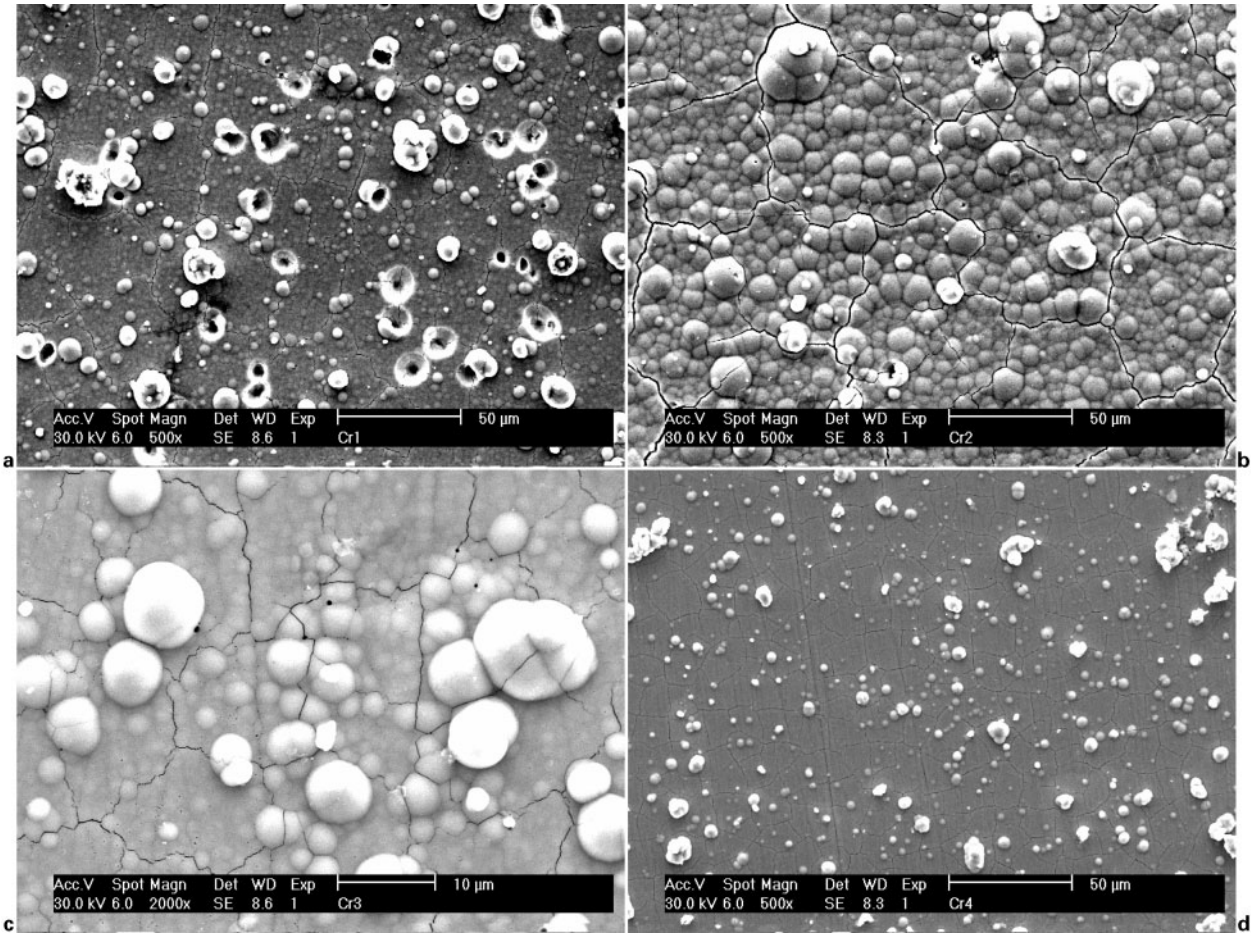

9 SEM image of Cr deposit from formate urea electrolyte *a* DC deposited Cr at 20 A dm^{-2} for 15 min, *b* DC deposited Cr at 20 A dm^{-2} for 30 min, *c* PC deposited Cr at 40% duty cycle and 25 Hz and *d* PC deposited Cr at 40% duty cycle and 10 Hz

The increased R_{ct} values and decreased C_{dl} values for Cr deposits clearly confirm the better corrosion resistance of these PC plating and DC deposition systems compared to bare mild steel substrates. Also it is observed a more pronounced semicircular region in the case of both PC plating and DC deposition of Cr indicting that the PC plating has more corrosion resistance than DC deposition, which is more corrosion resistance than mild steel as observed from the high frequency region of the impedance spectra. The corrosion rate *CR* is expressed in mills per year

$$CR = 0{\cdot}1288 \times I_{corr} \times w/\rho$$

where I_{corr} is corrosion current in Adm^{-2}, w is equivalent weight of metal and ρ is density.

The corrosion rate observed on PC and DC plated Cr was significantly lower than that of mild steel substrate. Corrosion behaviour of both PC and DC plated Cr is further illustrated by bode plot, where it can be seen that the mild steel has lowest absolute impedance. The $|z|$ value of the PC deposited Cr is significantly higher than DC plated Cr. Similarly the $|z|$ value of DC deposited Cr is higher than mild steel. This confirms that both PC and DC plated Cr provide better corrosion protection to the steel substrate. All these graphs are equivalent to a typical Randle's circuit.

Morphology of Cr deposit

Scanning electron microscopic studies

The surface morphology of Cr electrodeposited was significantly changed by pulse current. The SEM photomicrographs of Cr electrodeposits obtained from DC and PC plating are shown in Fig. 9. Figure 9*a* and *b* is the SEM photomicrograph of DC electrodeposited Cr at 20 A dm^{-2} for 15 and 30 min respectively. Both deposits have a large nodular size and microcracks. The microcracks form during electrodeposition when tensile stress exceeds the cohesive strength of the deposit. The higher the inhibition of lateral grain growth, the higher the nucleation rate and so the higher the number of grains that coalesce and main inhibiting species is the adsorbed hydrogen.

Figure 9*c* and *d* is the SEM photomicrographs of PC deposited Cr after 15 min of plating at pulse frequencies of 25 and 10 Hz. The applied average current density was 14 A dm^{-2}. Both deposits have a smaller nodular size. In the PC deposition; the peak current density is higher than average current density, which leads to a decreased grain size. The decreased porosity and denser packed surface are due to the desorption of hydrogen during the off-time of pulse cycle.

Atomic force microscopic studies

The AFM images of the deposits with a thickness of 10·5 and 10 µm are shown in Fig. 10*a* and *b*. Figure 10*a* is the DC Cr deposits at 15 A dm^{-2} with dispersed or dispersoids growth nodules.[21] The size of crystallites increases with increasing in thickness of coating and agglomerates formed by dispersoids are distinctly seen in the deposit with a thickness of about 10–16 µm. Figure 10*b* is the PC Cr deposits at 14 A dm^{-2} (AC) have a more fine grained structure without dispersoids in

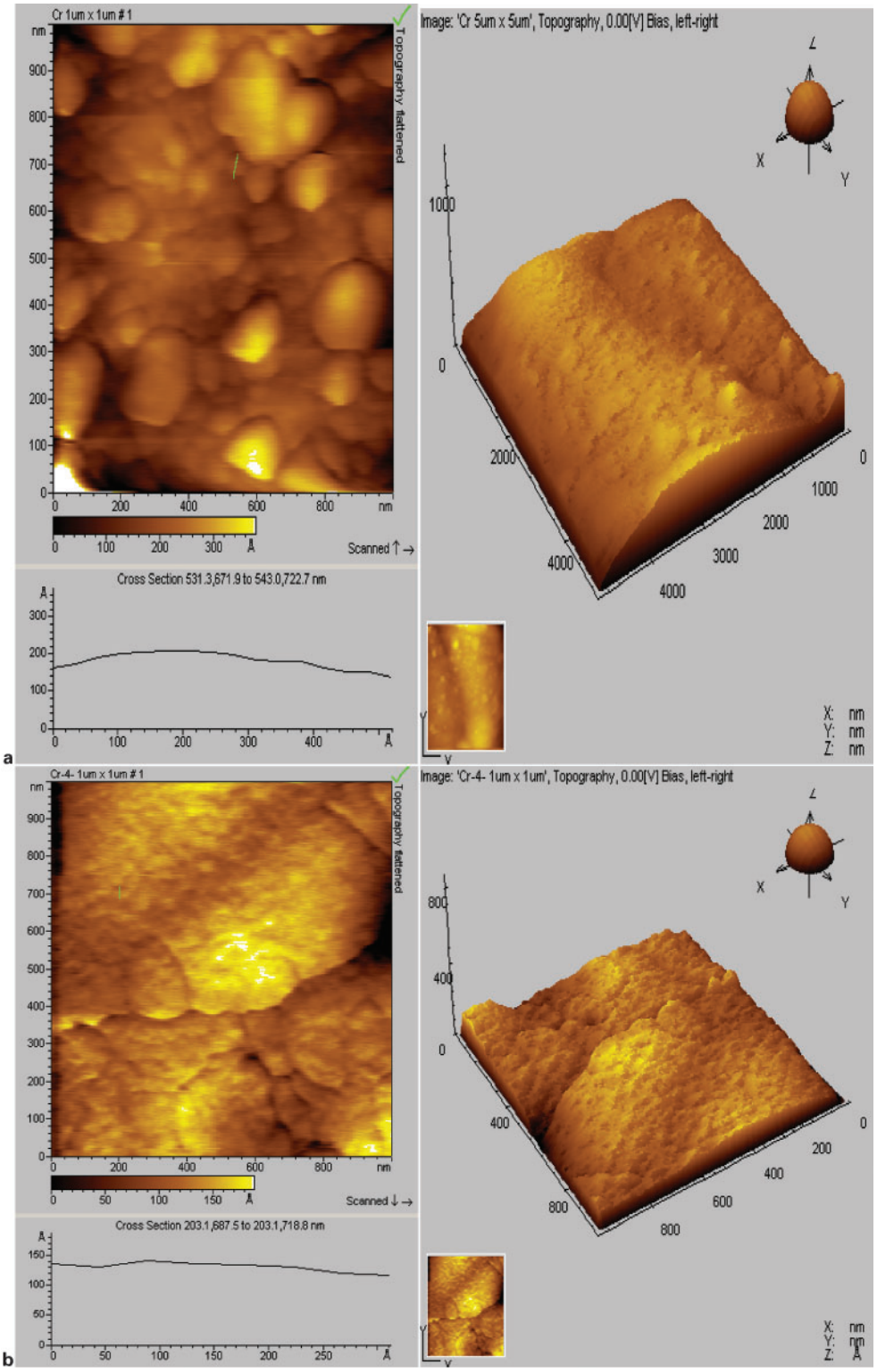

10 Atomic force microscopy of Cr deposit from formate urea electrolyte at *a* DC deposited Cr at 20 A dm^{-2} and *b* PC deposited Cr at 40% duty cycle and 10 Hz

comparison with those deposited in DC Cr deposits. The smaller grain size may be conditioned by progressive nucleation during on-time of PC deposition. The formation of numerous new nucleations sits as well as fine and smooth grained structure is formed.

X-ray diffraction studies

Chromium may be electrodeposited in various phases (α, β and γ phases).[22] The phases obtained are dependent on plating conditions. α-Chromium[23,24] is the most predominant and stable phases, however, β-Cr only deposited under certain conditions and converts eventually to α-Cr over time or with annealing. Figure 11A and B shows the XRD pattern of the Cr deposited and annealed at 400°C. The broad peak obtained at $2\theta=44{\cdot}05$ is amorphous Cr (110) and $2\theta=72{\cdot}15$, $2\theta=87{\cdot}41$ are the base metal copper (220) and (311) were obtained. The specimen was heated for 30 min, the

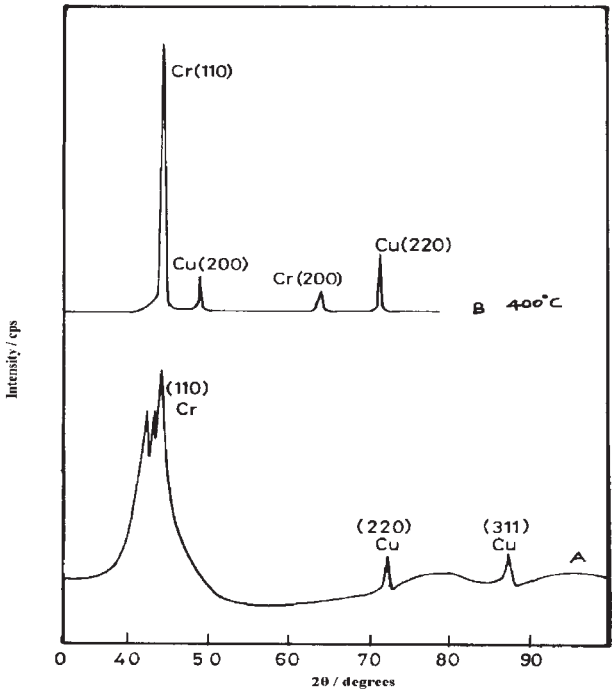

11 (A) X-ray diffraction pattern of DC plated Cr at 15 A dm^{-2} and (B) annealed XRD pattern of Cr at 400°C for 30 min

broad peak of Cr a (110) increased in intensity and replaced by sharp peaks of crystalline α-Cr at 400°C with $2\theta=44{\cdot}29$. However, the peak at $2\theta=64{\cdot}54$ is attributed to the presence of (200) plane of γ-Cr and $2\theta=49{\cdot}10$, $2\theta=72{\cdot}07$ are the base metal copper (200) and (220).[25]

The crystallite sizes of Cr coatings were calculated from the Scherer's equation

$$D=\frac{0{\cdot}94\lambda}{\beta\cos\theta} \quad (1)$$

where D is the grain size, β is the full width at half maximum (FWHM) of the diffraction peak, λ is the wavelength of the incidental X-ray (1·54 Å), and θ is the diffraction angle. Based on equation (1), the average crystallite sizes were found to be 26·75 Cr(110), 25·57 Cu(220) and 17·59 nm Cu(311) respectively.

Similarly for annealed Cr crystallite sizes were found to be 26·76 Cr(110), 54·52 Cu(200), 18·33 Cr(200) and 31·42 nm Cu(220) respectively.

Table 5 Texture coefficient obtained from XRD pattern of amorphous/microcrystalline Cr coating

hkl	2θ	*D*, Å	I/I_0	T_C (ø)
Cr (110)	44·05	2·05	1	70·73
Cu (220)	72·15	1·30	0·27	19·47
Cu (311)	87·46	1·11	0·13	9·78

Table 6 Texture coefficient obtained from XRD pattern of annealed Cr coating at 400°C for 30 min

hkl	2θ	*D*, Å	I/I_0	T_C (ø)
Cr 110	44·29	2·04	1	71·98
Cu 200	49·10	1·85	0·1326	9·54
Cr 200	64·54	1·44	0·0771	5·54
Cu 220	72·07	1·30	0·1795	12·92

The preferred growth orientation was determined using texture coefficient TC_{hkl}. This factor can be calculated by using

$$TC_{hkl}=I/I_0$$

$$1/N[(I/I_0)]$$

where TC_{hkl} is the texture coefficient of the plane, I_{hkl} is the measured intensity of the (hkl) plane, $I_{o(hkl)}$ corresponds to the recorded intensity in the JCPDS data file and N is the number of preferred directions of the growth. The TC_{110} was found to be 70·73 and annealed Cr TC_{110} was found to be 71·98. Data are given in Tables 5 and 6. This indicates that the Cr film has strong reflex along (110).

Conclusion

1. Amorphous/microcrystalline thick Cr coatings with acceptable quality were electrodeposited from trivalent Cr bath by DC and PC techniques. From the results obtained PC deposition is better than DC technique.
2. Annealing at 400°C resulted in the loss of the hydrogen gas from amorphous/microcrystalline which leads to the crystallisation of Cr
3. Corrosion measurements shows that PC and DC Cr deposited have better corrosion resistance than that of mild steel.
4. Scanning electron microscope and atomic force microscopy images of PC Cr deposits show finer grained nodular cracks free deposits than those of DC Cr deposits.

Acknowledgement

One of the authors (Dr S. Mohan) thanks the Department of Science and Technology New Delhi for a research grant under SERC (Engineering Sciences) scheme no. SR/S3/ME/047/2005.

References

1. J. C. Saiddington: *Plat. Surf. Finish.*, 1978, **65**, (1), 45–49.
2. G. A. Lausmann: *Surf. Coat. Technol.*, 1996, **87**, 814–820
3. J. H. Lindsay: *Plat. Surf. Finish.*, 1997, **84**, (9), 14–21.
4. Y. B. Song and D.-T. Chin: *Electrochim. Acta*, 2002, **48**, (4), 349–356.
5. S. K. Ibrahim, D. T. Gawne and A. Watson: *Trans. IMF*, 1998, **76**, (4), 156–161.
6. S. K. Ibrahim, A. Watson and D. Gawne: *Trans. IMF*, 1997, **75**, (5), 181–188.
7. J-Y. Hwang: *Plat. Surf. Finish.*, 1991, **78**, (5), 118–124.
8. M. El-Sharif, S. Ma and C. U. Chisholm: *Trans. IMF*, 1995, **73**, (1), 19–25.
9. M. El-Sharif, S. Ma and C. U. Chisholm: *Trans. IMF*, 1999, **77**, (4), 139–144.
10. L. N. Vykhodtseva, A. A. Edigaryan, E. N. Lubnin, Y. M. Polukarov and V. A. Sofonov: *Russ. J. Electrochem.*, 2004, **40**, (4), 387–393.
11. N. V. Mandich: *Plat. Surf. Finish.*, 1997, **84**, (5), 108–115.
12. Z.-M. Tu, Z.-L. Yang and J.-S. Zhang: *Plat. Surf. Finish.*, 1990, **77**, (10) 55–57.
13. G. Devaraj and S. K. Seshadri: *Plat. Surf. Finish.*, 1996, **83**, (6), 62–66.
14. B. S. Li, A. Lin, X. Wu, Y. M. Zhang and F. X. Gan: *J. Alloys Compd*, 2006, **453**, (1–2), 93–101.
15. T. G. Sitnikova and A. S. Sitnikov: *Protect. Met.*, 2003, **39**, (3), 241–244.
16. P. Leisner, G. Bech-Nielsen and P. Moller: *J. Appl. Electrochem.*, 1993, **23**, 1232–1236.
17. Z. X. Zeng, L. P. Wang, A. M. Liang and J. Y. Zhang: *Electrochim. Acta*, 2006, **52**, 1366–1373.

18. T. Pearson and J. K. Dennis: *J. Appl. Electrochem*., 1990, **20**, 196–208.
19. T. Pearson and J. K. Dennis: *Surf. Coat. Technol*., 1990, **42**, 69–79.
20. J. C. Puippe and F. Leaman: 'Theory and practice of pulse plating', 1st edn, 247; 1986, Orlando, FL, American Electroplaters and Surface Finishers Society.
21. S. Surviliene, O. Nivinskiene, A. Cesuniene and A. Selskis: *J. Appl. Electrochem.*, 2006, **36**, 649–654.
22. H. Dasarathy, C. Riley and H. D. Coble: *J. Electrochem. Soc*., 1994, **141**, 1773–1779.
23. D. Sherwood and B. Emmanuel: *Cryst. Growth Design*, 2006, **6**, 1415–1419.
24. H. Okada and T. Ishida: *Nature*, 1960, **187**, 496–497.
25. S. S. Abd El Rehim, M. A. M. Ibrahim and M. M. Dankeria: *Trans. IMF*, 2002, **80**, 29–33.